

High-Capacity Mode Division Multiplexing Transmission Technology

Daiki Soma, Shohei Beppu, Noboru Yoshikane and Takehiro Tsuritani

KDDI Research, Inc., 2-1-15 Ohara, Fujimino-shi, Saitama, 356-8502 Japan

da-souma@kddi-research.jp

Abstract: Mode division multiplexing is an attractive method of increasing the transmission capacity. This paper presents the 402.7-Tbit/s weakly coupled 10-mode-multiplexed transmission over 48 km and 50.47-Tbit/s standard cladding coupled 4-core fiber transmission over 9,150 km. © 2022 The Author(s)

1. Introduction

A space division multiplexing (SDM) transmission technique has been investigated as a means of overcoming the theoretical limitation of transmission capacity in a standard single-mode fiber (SMF). In particular, 125- μm standard cladding space-division multiplexing (SDM) fibers are attractive for early deployment in SDM systems since they are expected to have similarly high productivity and high mechanical reliability as the existing SMFs. In such SDM fibers, the mode-division multiplexing (MDM) technique [1-8] is useful to space-efficiently scale up the system capacities for future enormous traffic demands.

In a broad sense, two types of MDM technologies have been reported: the first one uses conventional multimode fibers (MMFs) and few-mode fibers (FMFs), and the second one uses coupled multicore fibers (MCFs). Figure 1 shows the relationship between the transmission distance and the transmission capacity in recent MDM transmission experiments using MMFs/FMFs and coupled MCFs. To date, 45-mode multiplexed transmission [1] using 90 \times 90 multiple-input multiple-output (MIMO) with graded-index conventional MMF and 1.01 Pbit/s transmission [2] using 30 \times 30 MIMO with 15-mode fiber have been reported. However, for the commercialization of MDM systems, it would be strongly necessary to reduce the complexity of MIMO processing. In this presentation, we report on weakly coupled 10-mode multiplexed transmission [3] with only 2 \times 2 and 4 \times 4 MIMO over a 48-km 125- μm cladding step index few-mode fiber. By using probabilistically shaped (PS) dual polarization (DP) 16 quadrature amplitude modulation (QAM) signals, we achieve a transmission capacity of 402.7 Tbit/s in the standard cladding SDM fiber.

On the other hand, coupled MCFs are expected to be applied to long-haul transmission assuming optical submarine cable systems, as shown in Fig. 1, because they have smaller mode-dependent loss (MDL) and spatial mode dispersion (SMD) than conventional MMFs and FMFs, although the number of spatial multiplexing is smaller. Recently, transoceanic distance transmissions have been reported with standard cladding coupled 4-core fibers [4] and coupled 7-core fibers [5]; however, the bandwidth used in these experiments is a part of the C-band and is smaller than 5 nm. In wide bandwidth transmission, the longest transmission distance was 5,500 km in a 34.56-Tbit/s transmission using a coupled 4-core fiber [6]. In this presentation, we also report on trans-Pacific class transmission [7] using standard cladding ultralow-loss coupled 4-core fibers, which achieved a transmission capacity of 50.47 Tbit/s after 9,150-km transmission.

2. Weakly coupled 10-mode multiplexed transmission

Weakly coupled MDM transmission with suppressed crosstalk (XT) between modes using lower-order MIMO processing has been proposed to mitigate the burden of MIMO processing in higher-order MDM transmissions [8]. In this section, we introduce weakly coupled 10-mode multiplexed transmission [3] with only a 2 \times 2 MIMO and 4 \times 4 MIMO over a 48-km 125- μm cladding 10-mode fiber (10MF) [9]. In this experiment, we measured the normalized generalized mutual information (NGMI) [10] for 10-mode-multiplexed 747-WDM 12-Gbaud PS-DP-16QAM signals

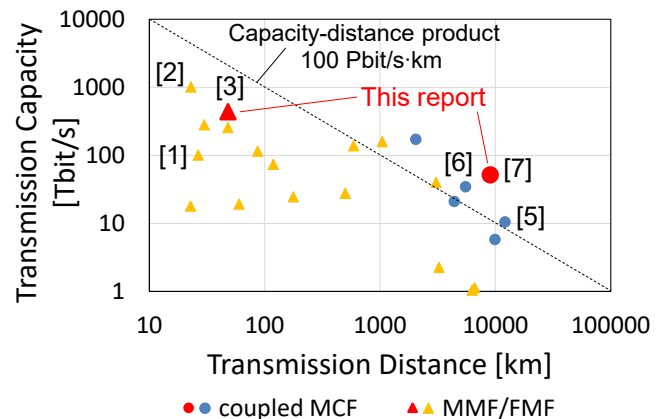


Fig. 1. Transmission distance vs. transmission capacity in recent MDM transmission experiments using MMFs/FMFs and coupled MCFs.

after 48-km weakly coupled 10MF transmission. The PS-16QAM signals were generated by using probabilistic amplitude shaping [11], and their entropies were optimized for each WDM channel to maximize the spectral efficiency. The 379 WDM channels (1527.459-1565.138 nm) in the C-band and 368 WDM channels (1569.851-1608.490 nm) in the L-band were modulated by the PS-16QAM signals. After these WDM signals were combined and power-equalized over the C+L-band, we obtained 12.5 GHz-spaced 12 Gbaud 747-WDM Nyquist-shaped PS-DP-16QAM signals. The generated WDM signals were fed into each port of a highly mode-selective 10-mode multiplexer. Ten modes, namely, LP01, LP11a, LP11b, LP21a, LP21b, LP02, LP31a, LP31b, LP12a, and LP12b, were generated and excited into the 10MF by the multiplane light conversion (MPLC) technique [12]. The average XT between the two modes and the total modal XT from the other LP modes in this 10-mode multiplexer/demultiplexer measured at 1550 nm were approximately -22.9 dB and -13.6 dB, respectively.

The transmission 10MF, which has a step-index-type profile, was designed with large differences ($> 6 \times 10^{-4}$) in the effective refractive index between adjacent LP modes to suppress the modal XT [9]. The core diameter and cladding diameter of the 10MF were 17 μm and 125 μm , respectively. In this transmission experiment, we optimized the launched signal power of each mode into individual input ports of the mode multiplexer across the C- and L-bands at 1550 nm and 1590 nm so that the differences of the measured NGMIs between the 10 modes caused by the differences of modal XT were equalized.

After 48-km transmission, the 10-mode multiplexed WDM signals were mode demultiplexed by the 10-mode demultiplexer and then wavelength demultiplexed by optical bandpass filters. Five demultiplexed lower-order modes (LP01, LP11a, LP11b, LP21a and LP21b) or five higher-order modes (LP02, LP31a, LP31b, LP12a and LP12b) were simultaneously detected by five coherent receivers based on heterodyne detection. In offline processing, the stored samples were independently processed by two adaptive 2×2 MIMO equalizers for LP01/LP02 and four 4×4 MIMO equalizers for LP11ab/LP21ab/LP31ab/LP12ab. The MIMO tap size was set at 350 for all the modes. The MIMO tap coefficients were updated based on the decision-directed least-mean square (DD-LMS) algorithm [13]. After the symbols were decoded, the NGMIs were measured [10].

In this experiment, the entropies of the WDM channels were roughly optimized zone by zone in the wavelength so that the worst NGMI in the 10 modes was close to the forward error correction (FEC) threshold. Here, we assumed an FEC with a 25.5% overhead [14] whose Q limit of 4.95 dB corresponds to the NGMI threshold of 0.8571. Figure 2(a) shows the entropy of each WDM zone. Finally, we measured NGMIs of the 10-mode multiplexed 747-WDM channels. Figure 2(b) shows the NGMIs of all the spatial and wavelength channels (7,470 channels). The NGMIs of the measured WDM/MDM tributaries exceed the FEC threshold of 0.8571. In this experiment, we achieved a transmission capacity of 402.7 Tbit/s with only 2×2 MIMO and 4×4 MIMO over 48-km weakly coupled 10MF.

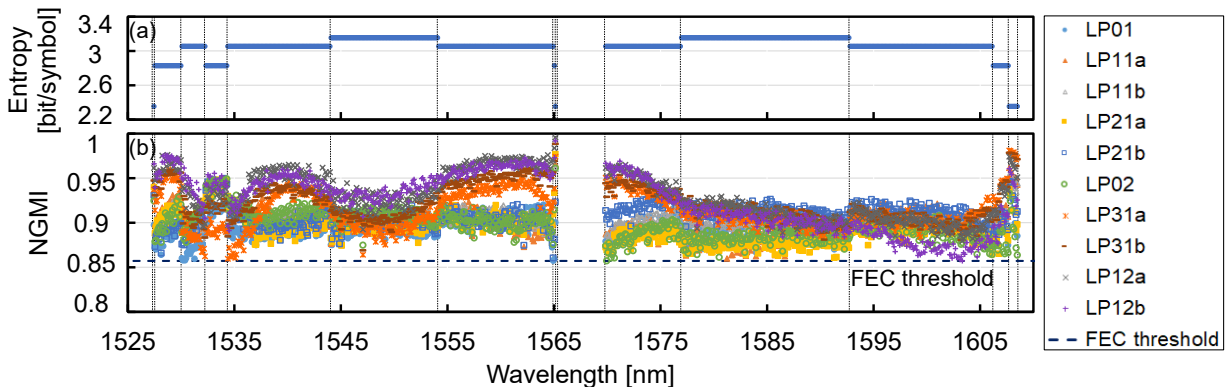


Fig. 2. (a) Entropy of each WDM channel and (b) measured NGMIs of all WDM/MDM tributaries.

3. Trans-Pacific class coupled 4-core fiber transmission

Coupled MCFs have been studied for long-haul transmission because they have lower MDL and SMD than conventional MMFs and FMFs. In this section, we introduce trans-Pacific class high-capacity MCF transmission [7] using standard cladding ultra-low-loss coupled 4-core fibers (4CFs) [15]. In this experiment, we measured the Q^2 factors of 608 (4 core \times 152 WDM) SDM/WDM channels after 9,150-km transmission. The 152 WDM channels (1534.545-1564.781 nm) in the C-band were modulated by 24-Gbaud Nyquist-shaped electrical two-level signals for QPSK (quadrature-phase-shift keying) signals. After these WDM signals were power-equalized over the C-band, we obtained 25 GHz-spaced 24 Gbaud 152-channel WDM Nyquist-shaped DP-QPSK signals. The generated WDM signal was split into 4 paths and fed into a recirculating loop system consisting of four spans of 60.2-km coupled 4CFs,

C-band EDFAs and 2×2 optical switches (SWs). The WDM signals after 4-span transmission were gain-equalized using four C-band WSSs. In this experiment, the skew between the four cores was compensated for each span via variable optical delay lines (VODLs).

The four cores arranged in a square lattice of the coupled MCF [15] have almost the same refractive index profile as an ultra-low-loss pure-silica-core single-mode fiber used for long-haul transmission. The core-averaged transmission loss, effective area, core pitch and SMD for the coupled MCF at 1550 nm were approximately 0.155 dB/km, 113 μm^2 , 20.2 μm and 7.1 ps/ $\sqrt{\text{km}}$, respectively. The insertion losses of the lens-coupled fan-out (FO) devices at 1550 nm ranged from 0.3 to 0.6 dB. In addition, the losses at one splice point were less than 0.1 dB. Therefore, in this experiment, the averaged total span losses were 11.8 dB, including VODLs with a typical insertion loss of 1.0 dB. As a preliminary experiment, we measured the Q^2 factors as a function of the power per channel for a 6,020-km transmission to determine the optimal fiber launch power in this coupled MCF using 16-WDM 24-Gbaud DP-QPSK signals. The highest Q^2 factor averaged among the four cores was obtained at -2 dBm/ch. Therefore, the signal powers launched into each core of the coupled 4CFs were also adjusted to -2 dBm/ch in this experiment.

The WDM signals transmitted 9,150 km were detected by four synchronized digital coherent receivers based on heterodyne detection after channel selection with optical bandpass filters. In offline processing, the stored samples were processed by an adaptive 8×8 MIMO equalizer with up to 500 taps. The MIMO tap coefficients were updated based on a DD-LMS algorithm [13]. After the symbols were decoded, the Q^2 factors were calculated.

Figure 3 shows the Q^2 factors of 608 SDM/WDM channels. In this experiment, we assumed a rate-adaptive FEC [16], which is a promising technology used to maximize system capacity with the OSNR and the nonlinear effect variation between WDM channels. Three different FECs with a 12.75% overhead (OH) and 6.5 dB FEC limit [17], a 20% OH and 5.7 dB FEC limit [18], and a 25.5% OH and 4.95 dB FEC limit [14] were employed, and one of them was selected for each channel according to the measured Q^2 factors. As shown in Figure 3, the Q^2 factors of 107 WDM channels, 19 WDM channels, and 26 WDM channels exceeded the thresholds of 12.75% OH FEC, 20% OH FEC, and 25.5% OH FEC, respectively. From the obtained experimental results, a transmission capacity of 50.47 Tbit/s (12.62 Tbit/s/core) was achieved using the 152-WDM 24-Gbaud DP-QPSK signals after a 9,150-km transmission by assuming the rate-adaptive FEC.

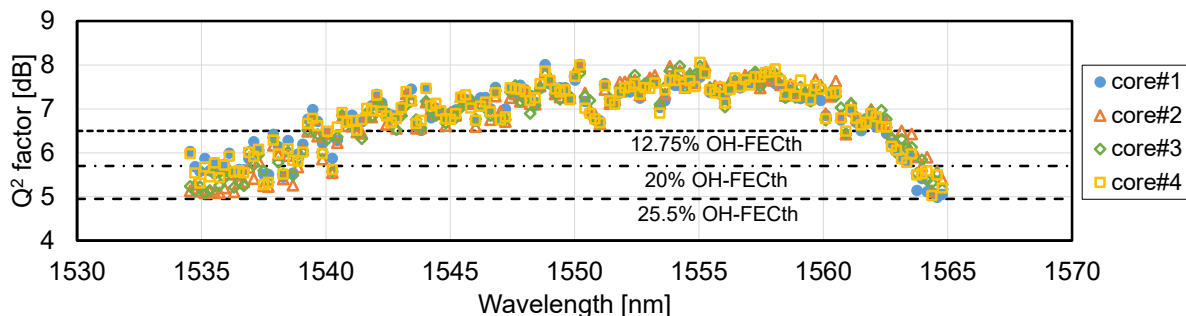


Fig. 3. The Q^2 factors of 608 SDM/WDM channels calculated from the measured BERs.

4. Conclusions

This paper presented weakly coupled 10-mode fiber transmission and trans-Pacific class coupled 4-core fiber transmission using two MDM technologies in a broad sense. In these experiments, we achieved a transmission capacity of 402.7 Tbit/s with only 2×2 MIMO and 4×4 MIMO over 48-km weakly coupled 10MF and 50.47 Tbit/s over 9,150-km standard cladding ultra-low-loss coupled 4CFs.

This work was partially supported by the Ministry of Internal Affairs and Communications (MIC)/Research and Development of Innovative Optical Network Technology for a Novel Social Infrastructure (JPMI00316) (Technological Theme II: OCEANS), Japan.

5. References

- [1] R. Ryf, *et al.*, ECOC2018, Th3B.1, (2018).
- [2] G. Rademacher, *et al.*, ECOC2020, Th3A-1, (2020).
- [3] D. Soma, *et al.*, ECOC2019, W.2.A.2, (2019).
- [4] D. Soma, *et al.*, ECOC2020, Mo2E.4, (2020).
- [5] R. Ryf, *et al.*, OFC2019, Th4B.3, (2019).
- [6] R. Ryf, *et al.*, ECOC2016, Th.3.C.3, (2016).
- [7] D. Soma, *et al.*, OFC2021, W7D.3, (2021).
- [8] C. Koebele, *et al.*, ECOC2011, Th13.C.3, (2011).
- [9] Y. Wakayama, *et al.*, OECC2017, 3-1K-4, (2017).
- [10] J. Cho, *et al.*, ECOC2017, M.2.D.2, (2017).
- [11] F. Buchali, *et al.*, JLT, **34**, (7), 1599, (2016).
- [12] G. Labroille, *et al.*, OFC2016, Th3E.5, (2016).
- [13] Y. Mori, *et al.*, OFC2012, OT4C.4, (2012).
- [14] K. Sugihara, *et al.*, OFC2013, OM2B.4, (2013).
- [15] H. Sakuma, *et al.*, ECOC2019, M.1.D.2, (2019).
- [16] D. Zou, *et al.*, Optics Express, **24** (18), 21159, (2016).
- [17] T. Kobayashi, *et al.*, OFC2017, Th5B.1, (2017).
- [18] D. Chang, *et al.*, OFC2012, OW1H.4, (2012).